International Journal of Pharmaceutics 430 (2012) 266–275

Contents lists available at SciVerse ScienceDirect

International Journal of Pharmaceutics

journal homepage: www.elsevier.com/locate/ijpharm

Pharmaceutical Nanotechnology

Temozolomide loaded PLGA-based superparamagnetic nanoparticles for magnetic resonance imaging and treatment of malignant glioma

You Ling[a,b,c], Kun Wei[a,b,c,*], Fen Zou[a,b,c], Shizheng Zhong[a,b,c]

[a] School of Materials Science and Engineering, South China University of Technology, Guangzhou, Guangdong 510640, China
[b] National Engineering Research Center for Human Tissue Restoration and Function Reconstruction, Guangzhou, Guangdong 510006, China
[c] Guangdong Province Key Laboratory of Biomedical Engineering, South China University of Technology, Guangzhou, Guangdong 510006, China

ARTICLE INFO

Article history:
Received 12 January 2012
Received in revised form 29 February 2012
Accepted 25 March 2012
Available online 31 March 2012

Keywords:
Polysorbate 80
Temozolomide
PLGA
Superparamagnetic nanoparticles
MRI
Brain glioma

ABSTRACT

Polysorbate 80 coated temozolomide-loaded PLGA-based superparamagnetic nanoparticles (P80-TMZ/SPIO-NPs) were successfully synthesized and characterized as drug carriers and diagnosis agent for malignant brain glioma. The mean size of P80-TMZ/SPIO-NPs was 220 nm with narrow hydrodynamic particle size distribution. The superparamagnetic characteristic of P80-TMZ/SPIO-NPs was proved by vibration simple magnetometer. P80-TMZ/SPIO-NPs exhibited high drug loading and encapsulation efficiency as well as good sustained drug release performance for 15 days. MTT assay demonstrated the antiproliferative effect of P80-TMZ/SPIO-NPs for C6 glioma cells. Significant cellular uptake of P80-TMZ/SPIO-NPs was evaluated in C6 glioma cells by fluorescence microscopy, Prussian blue staining, and atomic absorption spectrophotometer (AAS) for qualitative and quantitative study, respectively. MRI scanning analyses in vitro indicated that P80-TMZ/SPIO-NPs could be used as a good MRI contrast agent. Polysorbate 80 coated temozolomide-loaded PLGA-based superparamagnetic nanoparticles could be able to promise a multifunctional theragnostic carrier of brain cancer.

1. Introduction

Brain cancer is a profound and unsolved clinical problem because of late diagnosis and the limitations of conventional therapies. The physiology of brain presents unique challenges, including of tight entering the brain space, limited distribution of substances along extracellular fluid flow pathways, and clearance from the tissue (Szoka et al., 2006; Rozhkova, 2011; Invernici et al., 2011). To overcome these problems, several strategies were developed to approach for effective brain drug delivery such as chimeric peptide, cationic proteins, prodrug, liposome, and nanoparticles (NPs). Among the various approaches, NP carriers, particularly polymeric NPs, seem to be the most interesting strategy (Kanwar et al., 2009). Biodegradable polymeric NPs possess many advantages such as the increase in drug reaching its target, enhanced selectivity, and the potential for delivery of multiple agents at the same site. Moreover, these carriers show a higher stability in biological fluids and against the enzymatic metabolism than colloidal carrier instances of the liposome or lipidic vesicles (Labhasetwar and Panyam, 2003).

Recently, theragnostics, the fusion of therapeutic and diagnostic approaches, has potential to be a kind of personalize and advance medicine. The multifunctional NPs platform would become an ideal strategy for theragnostics due to their diagnostic and therapeutic capabilities (Zhang et al., 2008; Dai et al., 2011; Xu et al., 2011). Drug loaded superparamagnetic NPs is a kind of multifunctional NPs platform, which has the preponderances including passively targeted by the enhanced permeability and retention, actively targeted under the aid of an external magnetic field, and rendering visible in magnetic resonance imaging (MRI) by reducing both T1 and T2/T2* relaxation times. Therefore, several scientific research groups are interesting to study the drug loaded superparamagnetic NPs. For examples, Kim et al. reported a nucleolin-targeted multimodal nanoparticle imaging probe for tracking cancer cells by using a gene drug (Kim et al., 2010). Haam et al. developed pH-sensitive drug-delivering magnetic nanoparticles as theragnostic nanocarriers that release doxorubicin under acidic conditions within cancer cells (Suh et al., 2011). Zhang et al. designed a novel multifunctional polymeric nanoparticles contrast agent simultaneously modified with gadolinium-diethylenetriamine pentaacetic acid (Gd-DTPA) and anti-vascular endothelial growth factor antibody to deliver Gd-DTPA to the tumor area and achieve the early diagnosis of hepatocellular carcinoma (Zhang et al., 2011). Cheng et al. developed multifunctional nanoparticles with highly integrated functionalities including upconversion luminescence, superparamagnetism, and strong optical absorption in the near-infrared region

* Corresponding author at: School of Materials Science and Engineering, South China University of Technology, Guangzhou, Guangdong 510640, China.
Tel.: +86 20 39380098; fax: +86 20 39380098.
E-mail address: weikun@scut.edu.cn (K. Wei).

0378-5173/$ – see front matter © 2012 Elsevier B.V. All rights reserved.
http://dx.doi.org/10.1016/j.ijpharm.2012.03.047

with high photostability for imaging-guided, magnetically targeted physical cancer therapy (Cheng et al., 2012).

The blood–brain barrier (BBB) is a major factor to restrict intracranial therapeutic effect because of the limited permeability of certain drug molecules within the brain which prevent the diffusion of these agents into the brain tumor. Many researches showed that NPs coated with polysorbate 80 could assist the therapeutic agents to across this barrier into the brain, which were normally cannot cross the BBB (Ruan et al., 2011; Bojat et al., 2011). Temozolomide (TMZ) is one of the most effective antineoplastic agents for malignant glial tumor, partially due to its ability to cross the BBB (Reni et al., 2004). However, the short half-life time of TMZ is about 1.8 h in plasma on the clinical application. Furthermore, prolonged systemic administration is associated with some side effects such as nausea, vomiting, fatigue and headache (Gaya et al., 2002).

In this study, we applied a well-known biodegradable polymer poly(D,L-lactide-co-glycolide) (PLGA) to be matrical material, which has long history of safe use in pharmaceutical and approved in medical applications by FDA. Then we prepared TMZ loaded superparamagnetic NPs and coated with polysorbate 80. The physicochemical property of formulated NPs was characterized by different techniques such as transmission electron microscopy and dynamic laser light scattering. Furthermore, we investigated the multifunctional NPs by the cytotoxicity assay, cellular uptake and MRI scanning in vitro. Polysorbate 80 coated temozolomide-loaded PLGA-based superparamagnetic nanoparticles (P80-TMZ/SPIO-NPs) were evaluated the feasibility for both MRI contrast agent and cancer therapy in brain glioma C6 cells.

2. Materials and methods

2.1. Materials

Poly(lactide-co-glycolide) acid (PLGA, L:G molar ratio = 50:50, Mw: 30,000), temozolomide (TMZ) and polysorbate 80 (Tween 80) were purchased from Sigma Chemical Co. (USA). Vitamin E D-α-tocopherol polyethylene glycol 1000 succinate (TPGS) was from Eastman chemical company (USA). Cell culture media and fetal bovine sera (FBS) were obtained from GIBCO, Invitrogen Corporation (Carlsbad, CA, USA). Other chemicals and solvents used in this study were of analytical grade.

2.2. Nanoparticles preparation

2.2.1. PLGA-based NPs preparation

Superparamagnetic iron oxide (SPIO) was synthesized in our laboratory as described in the previously reported method (Ling et al., 2011). TMZ-loaded PLGA-based superparamagnetic NPs (SPIO/TMZ-NPs) were prepared using the emulsifying-solvent evaporation method. Briefly, a definite amount of TMZ (10–80 mg) and 100 mg PLGA were dissolved in 2 ml dimethylformamide (DMF), and then 20 mg SPIO was added. The organic phase was slowly poured into 50 ml 0.05% (w/v) TPGS aqueous solution and emulsified using micro-tip probe sonicator in pulse mode for 5 min. The resulted oil-in-water emulsion was agitated overnight at room temperature to allow the organic solvent to evaporate. The suspension was centrifuged at 1000 rpm to remove agglomeration and then separated by a magnet. SPIO/TMZ-NPs were dispersed in specified volume of solution for subsequent experiments.

2.2.2. Polysorbate 80 coated with SPIO/TMZ-NPs

Polysorbate 80 coating of SPIO/TMZ-NPs formulation was performed as the procedure described by Wilson et al. (2008). Typically, SPIO/TMZ-NPs were resuspended in phosphate buffered saline at a concentration of 20 mg/ml under constant stirring. Then polysorbate 80 was added to give a final solution of 1% polysorbate 80, and the mixture was incubated for 30 min. P80-TMZ/SPIO-NPs were collected by magnetic separation technology and finally lyophilized. For contrast test, the polysorbate 80 coated PLGA-based superparamagnetic NPs (P80-SPIO-NPs) were prepared without loading TMZ. The Tween 80 coated TMZ-loaded PLGA-based NPs (P80-TMZ-NPs) were prepared without loading SPIO. For imaging, the polysorbate 80 coated rhodamine/coumarin-loaded PLGA-based superparamagnetic NPs (P80-RC/SPIO-NPs) and rhodamine/coumarin-loaded PLGA-based superparamagnetic NPs (RC/SPIO-NPs) were synthesized using rhodamine or coumarin instead of TMZ.

2.3. Characterization of nanoparticles

2.3.1. Particle size, size distribution and morphology

Average particle size and size distribution of NPs were measured by dynamic laser light scattering (DLS, Zetasizer Nano ZS, Malvern Instruments, UK). The samples were diluted with deionized water and sonicated for several minutes before measurement. The data were obtained by the average of triple measurements. The shape and surface morphology of P80-TMZ/SPIO-NPs were investigated by transmission electron microscope (TEM, JEM-2010HR, JEOL, Japan) and field emission scanning electron microscopy system (SEM, Nova Nano 430, FEI, Netherlands). For TEM, the NPs suspension was deposited on a copper grid covered with a formal-carbon membrane. For SEM, the NPs were fixed on the stub with a double-sided sticky tape and then coated with gold layer, which was carried out by an Auto Fine Coater (MSP-1S, Japan) for 30 s.

2.3.2. Vibration sample magnetometer

A VSM-BS2-11 Tesla was used to study the magnetic properties of P80-TMZ/SPIO-NPs. The SPIO synthesized in the lab was used as the control sample. The field dependence of magnetization was recorded at 10 K and 300 K under circulate magnetic field ranged between −2 T and 2 T. The temperature dependence of the magnetization was also investigated. The sample was cooled down to 10 K at a magnetic field of 2 T, and then measured the magnetic moment at a series of intermediate temperatures up to 300 K.

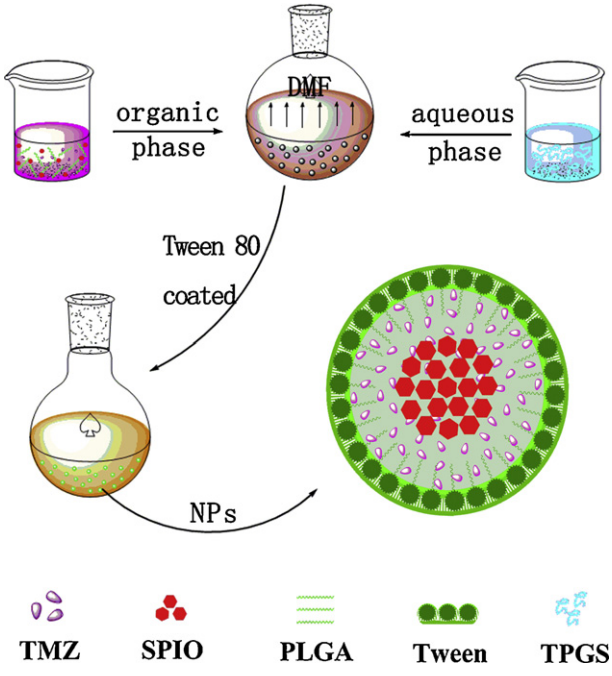

Fig. 1. Schematic representation of P80-TMZ/SPIO-NPs and the progress of formulation.

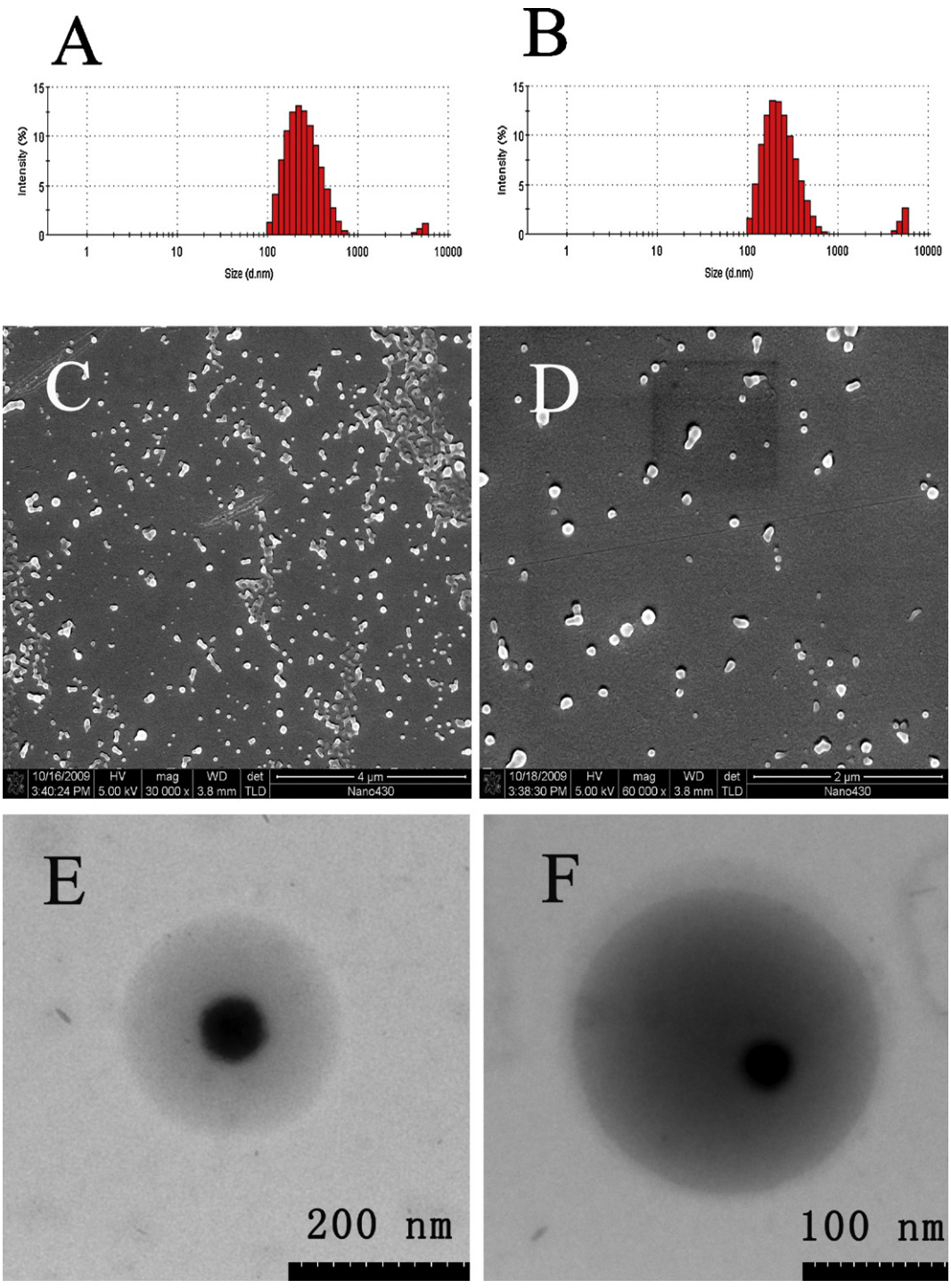

Fig. 2. Particle size and distribution of SPIO/TMZ-NPs (A) and P80-TMZ/SPIO-NPs (B) measured by DLS. SEM micrograph of SPIO/TMZ-NPs (bar = 4 μm) (C) and P80-TMZ/SPIO-NPs (bar = 2 μm) (D). TEM micrograph of SPIO/TMZ-NPs (bar = 200 nm) (E) and P80-TMZ/SPIO-NPs (bar = 100 nm) (F).

2.4. Drug loaded efficiency and in vitro release study

The TMZ drug loading contents (DL) and encapsulation efficiency (EE) of P80-TMZ/SPIO-NPs were determined in triplicate by UV–vis spectrophotometer at λ_{max} 327 nm. The lyophilized NPs were accurately weighed and dissolved in a certain volume of DMF via sonication till complete solubility. The DL was defined as the percentage of the actual drug mass in the NPs, and the EE was defined as the percentage of the actual mass of drug encapsulated in the polymeric carrier relative to the initial amount of drug loaded (Lee et al., 2005). In vitro release of P80-TMZ/SPIO-NPs was measured in phosphate buffered saline (PBS, pH 7.4) in triplicate at 37 °C. 5 mg P80-TMZ/SPIO-NPs were suspended in 10 ml of PBS in a screw capped tubes, which were placed in an orbital shaker bath and shaken horizontally at 120 rpm. At the specific time during incubation, samples were taken out and separated by magnetic technology. The supernatant was withdrawn and the NPs were dissolved in DMF. Due to the unstability of TMZ in the release test

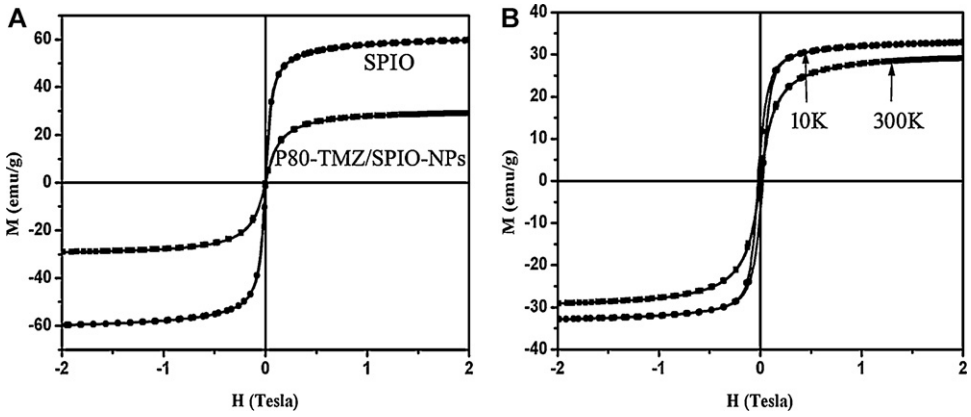

Fig. 3. (A) The magnetic behavior of SPIO nanocrystals and P80-TMZ/SPIO-NPs (300 K). (B) The temperature influence on P80-TMZ/SPIO-NPs.

condition, the amount of TMZ released into PBS was calculated by the amount of TMZ remained in the NPs at the specific release test periods (Huang et al., 2008).

2.5. Cell line experiment

2.5.1. Cell culture

Glioma C6 cell lines were obtained from American Type Culture Collection (ATCC, Manassas, VA). C6 cells were respectively cultivated in Dulbecco's modified Eagle medium (DMEM) and supplemented with 10% FBS and 1% penicillin–streptomycin at 37 °C in moist environment of 5% CO_2. The medium was replenished every other day and the cells were collected by trypsinization using 0.25% Trypsin-EDTA solution.

2.5.2. Cytotoxicity assay

The cytotoxicity of NPs against C6 cells was evaluated by using MTT assay. The cell viability was determined by a microplate reader. Glioma C6 cells were seeded in 96-well plates (Costa, Corning Incorporated) at the density of 5×10^3 cells per well and incubated 12 h to permit of cell attachment. Then the medium was changed with 200 μl medium with TMZ, P80-TMZ-NPs, and P80-TMZ/SPIO-NPs at equivalent drug concentrations ranging from 12.5 to 400 μg/μl and incubated for 24, 48 and 72 h. The following procedure was the same as common MMT assay method. Cell inhibition rate was calculated by the following equation:

$$\text{cell inhibitation rate } (\%) = \frac{A_{\text{control}} - A_{\text{drug}}}{A_{\text{control}} - A_{\text{blank}}} \times 100$$

where A_{drug} is the absorbance of the cells incubated with the free Dtxl or P80-SPIO-NPs or P80-TMZ/SPIO-NPs; A_{control} is the absorbance of the cells incubated with the culture medium only, and A_{blank} is the absorbance of the culture medium. All experiments were performed in triplicate.

2.5.3. Cellular uptake of NPs

For qualitative study, C6 cells were seeded on the chambers (Lab-Tek® Chambered Coverglass System) at a density of 2×10^4 cells per well. After 12 h incubation, the adherent cells were washed twice with PBS. Then the cells were treated with rhodamine/coumarin-6 labeled P80-RC/SPIO-NPs suspension (500 μl, 300 μg/ml) and further incubated for 2 h. Cells were washed four times and fixed with 4% paraformaldehyde for 20 min. Finally, the hoechst was added to stain the nucleus. The cell monolayer was washed twice with PBS and observed by fluorescence inverted microscope (Eclipse Ti-U, Nikon, Japan).

For quantitative study, C6 cells were seeded into 24-well black plates (Costar, IL, USA) at 2×10^4 cells per well. After the cells reached about 80% confluence, the medium was changed by the suspension of fluorescence labeling P80-RC/SPIO-NPs suspension at a NP concentration of 200 μg/ml and incubated for 0.5, 1.0, 2.0, 4.0 h, respectively. Moreover, the different NP concentrations from 0 to 400 μg/ml incubated for 2 h were investigated. RC/SPIO-NPs suspension was taken to the same incubation as contrast. After incubation, the NPs suspension was removed and the wells were washed three times with PBS. Then 200 μl 0.5% Triton X-100 in 0.2 N NaOH was added to the sample wells to lyse the cells. The fluorescence intensity present in each well was finally measured by microplate reader with excitation wavelength at 476 nm and emission wavelength at 582 nm for rhodamine and with excitation wavelength at 430 nm and emission wavelength at 485 nm for coumarin-6. The cellular uptake was expressed as the percentage of the fluorescence of the sample wells versus that of the positive control solution (Feng and Pan, 2008).

2.5.4. Prussian blue staining and intracellular Fe concentration

The intracellular ferric iron was measured by the Prussian blue staining experiment. C6 cells were seeded in 6-well plates (Costa, Corning Incorporated) at the density of 2.0×10^5 cells per well and incubated for 24 h. Then the medium was changed and continued to incubate for 2 h with P80-TMZ-NPs or SPIO/TMZ-NPs or P80-TMZ/SPIO-NPs at 80 μg/ml of Fe concentration. Subsequently, cells were washed with PBS for three times. After fixation by 2 ml 4% paraformaldehyde solution for 20 min, cells were incubated at 37 °C with 2 ml Prussian blue solution comprising equal volume of 2% hydrochloric acid aqueous solution and 2% potassium ferrocyanide (II) trihydrate for 30 min. Cells were washed thrice

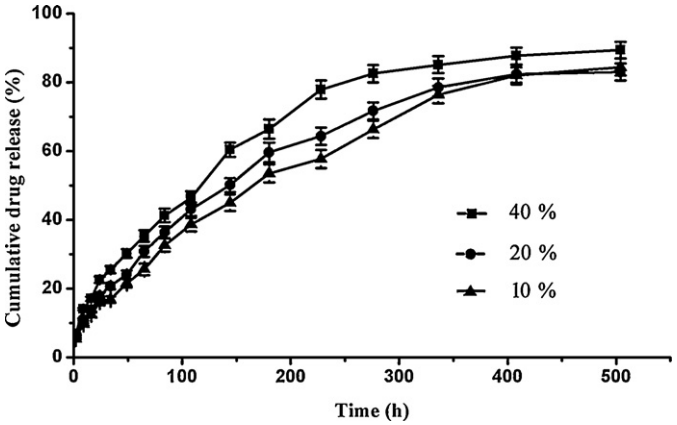

Fig. 4. (A) Release of TMZ in vitro from P80-TMZ/SPIO-NPs with 10%, 20%, and 40% drug loading. Data as mean ± s.e.m. ($n = 3$).

Table 1
Influence of the initial TMZ amount on encapsulation efficiency (EE), drug content (DL) and nanoparticles size (NPs size) using different methods that aqueous phase saturated or unsaturated with TMZ.

Method	TMZ (mg)	EE (%)	DL (%)	NPs size (nm)
Aqueous phase saturated with TMZ	10	77.68	7.21	218
	20	81.34	13.99	223
	40	89.78	26.43	220
	80	50.20	28.65	222
Aqueous phase unsaturated with TMZ	10	1.54	0.15	215
	20	6.71	0.40	217
	40	16.08	6.04	221
	80	27.35	17.95	219

and finally observed using a light microscope at the magnification of 200. For quantitative study, cells were treated as same as the preceding till fixation with paraformaldehyde. C6 cells were collected and treated with ultrasonication. The oxide iron was further decomposed with HNO_3 and H_2O_2. The constant volume clear solution gained, and the Fe concentration of intracellular uptake NPs was measured by atomic absorption spectrophotometer (AAS, Z-2000, Hitachi, Japan).

2.6. In vitro MRI

C6 cells, at the density of 1×10^6 cells, were washed and trypsinized after incubation with P80-TMZ/SPIO-NPs or Endorem® (a commercial contrast, Guerbet, France) at final Fe concentration of 0, 5, 10, 20, 40, 60, 80, and 100 μg/ml. After incubation for 2 h, cells were collected by trypsinization and centrifugation, and then resuspended in 1 ml 2% paraformaldehyde-containing PBS solution, followed by incubation at 4 °C for 1 h. Then cells suspension was centrifuged and washed with PBS to remove paraformaldehyde. 50 μl of 2% agarose solution (Type VII A) was added to fix the cells. Cells were scanned under a 1.5 T MRI scanner (Philips Intera, Netherlands, B.V.) at room temperature. The MRI T2 signal intensities within the region of interest were measured. T2 or T2*-weighted images were acquired under the following parameters: fast spin-echo (TSE), TR/TE = 5000/100 ms, Flip = 90°, FOV = 80 mm, matrix = 256 × 256, slice thickness = 1.5 mm, no. of echoes = 8 or gradient-recalled echo (FFE), TR/TE = 23/700 ms, Flip = 18°, FOV = 80 mm, matrix = 256 × 256, slice thickness = 1.5 mm, no. of echoes = 8.

3. Results and discussion

3.1. Nanoparticle preparation and characterization

TMZ-loaded PLGA based NPs were prepared using emulsifying-solvent evaporation method as described in Fig. 1. Since TMZ has a high solubility in the water and decompose easily when the pH of solution is above 7, in this preparation progress, aqueous phase containing 0.05% TPGS (pH 5) was saturated with TMZ beforehand to improve the EE of TMZ. It was reported that when aqueous phase was not saturated with TMZ, TMZ in the organic phase was almost diffused into the aqueous phase and the EE was only about 30% (Gao and Zhang, 2007). Table 1 shows the EE and DL of P80-TMZ/SPIO-NPs using different method. It was found that the EE was significantly improved when aqueous phase was saturated with TMZ as the same previously reported. The EE and DL were increased along with the initial TMZ amount from 10 to 40 mg. However, the EE was decreased to 50.2% when the amount of TMZ increased to 80 mg. It may be due to the low solubility of TMZ in DMF and weak miscibility with PLGA. Even the TMZ in the aqueous phase was saturated, TMZ in the DMF wound still diffuse into the aqueous phase and then formed the TMZ crystalline until that the organic phase solubility limit was stabilized. Therefore, the EE decreased as drug loading increased when the DL reached a certain amount.

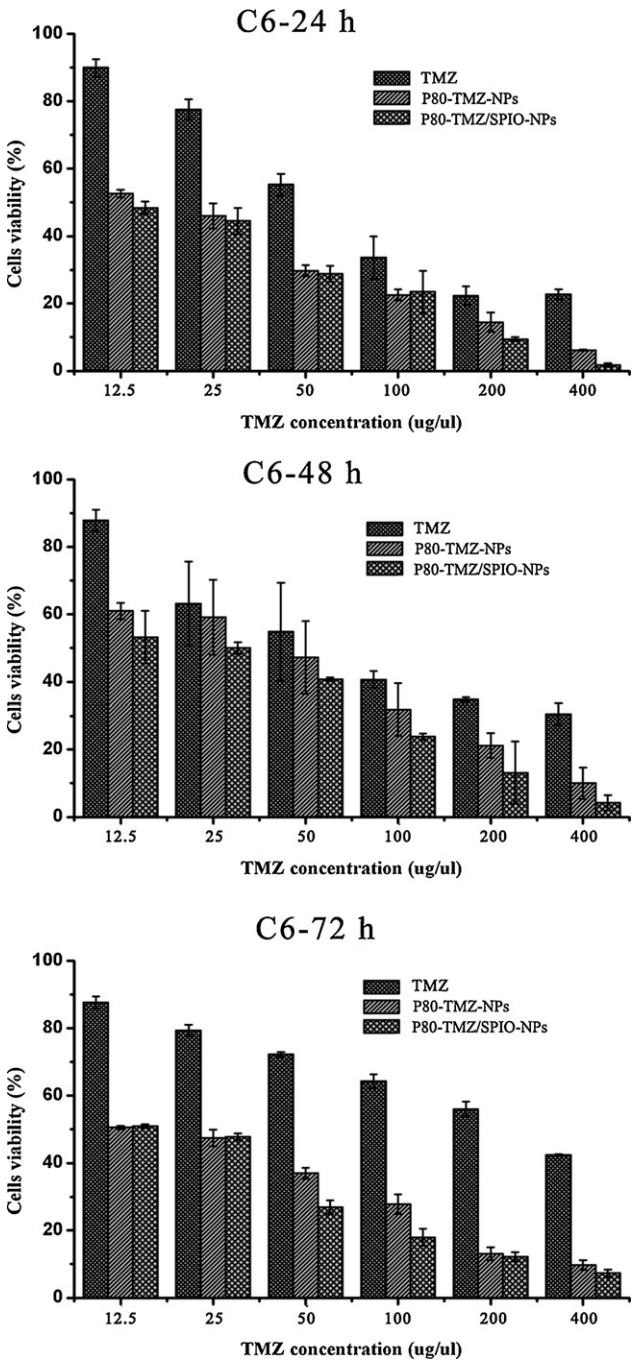

Fig. 5. In vitro assessment of the antiproliferative effects in C6 cells. The cells were incubated with TMZ or P80-TMZ-NPs or P80-TMZ/SPIO-NPs at equivalent drug concentrations ranging from 12.5 to 400 μg/μl for 24, 48 and 72 h. The cytotoxicity was evaluated by the MTT assay.

The sizes of the NPs were not appreciable impact with the different presence of drug. But the size of P80-TMZ/SPIO-NPs increased a little more than that of SPIO/TMZ-NPs. It was attributed to the surface coated with polysorbate 80. The mean size was increased from 197 nm to 220 nm (Fig. 2A and B). The size distribution was 0.114 and 0.131, respectively. SEM observations showed that SPIO/TMZ-NPs and P80-TMZ/SPIO-NPs were spherical and exhibited smooth surface (Fig. 2C and D). SPIO/TMZ-NPs appeared some more conglutination and the worse dispersibility than P80-TMZ/SPIO-NPs

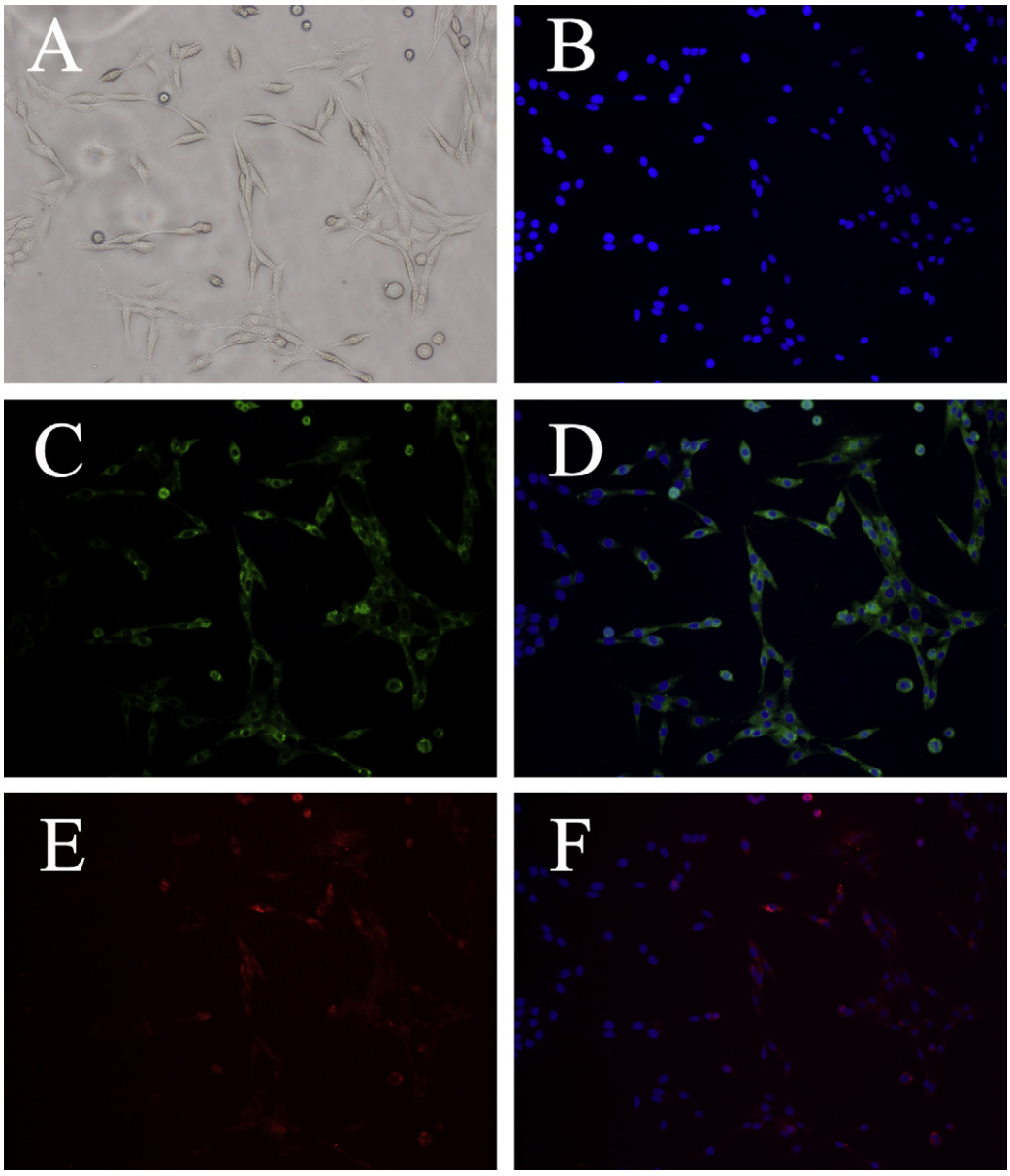

Fig. 6. Fluorescence inverted microscopy of C6 cells (2×10^4) incubated for 2 h with P80-RC/SPIO-NPs and labeled by rhodamine and coumarin-6. The hoechst was added to stain the nucleus. (A) Optical microscopy of C6 cells after incubation with P80-RC/SPIO-NPs; (B) blue fluorescent microscopy of C6 cells labeled the nucleus; (C) green fluorescent microscopy of C6 cells labeled the NPs by coumarin-6; (D) the composition fluorescent microscopy of blue and green fluorescent microscopy; (E) red fluorescent microscopy of C6 cells labeled the NPs by rhodamine; (F) the composition fluorescent microscopy of blue and red fluorescent microscopy. (For interpretation of the references to color in this figure legend, the reader is referred to the web version of the article.)

due to no surface modification with polysorbate 80. P80-TMZ/SPIO-NPs had no noticeable pinholes, tiny pores or cracks on the surface. TEM photograph showed that SPIO was effectively incorporated into polymer core (Fig. 2E and F). The polysorbate 80 coating on the PLGA-based NPs surface may be seen indistinctly.

3.2. Magnetization study

The magnetic properties of P80-TMZ/SPIO-NPs under a magnetic field were evaluated by VSM in order to confirm the potential and sensitivity as MR imaging nanoprobes. Fig. 3A shows that P80-TMZ/SPIO-NPs exhibited superparamagnetism without magnetic hysteresis at room temperature (300 K). The saturation magnetization value of P80-TMZ/SPIO-NPs at 2 T was 29.1 emu/g. Comparatively, it was much lower than the value of SPIO 60.5 emu/g. It was attributed to the non-magnetic PLGA and TW polymer matrix. However, this value of P80-TMZ/SPIO-NPs still has a higher saturation magnetization value than the previous report by other group such as 7.3 emu/g (Neoh et al., 2006) and 14 emu/g (Fessi et al., 2007), in order that it was satisfied for clinical application. Fig. 3B shows the magnetic field dependence of the P80-TMZ/SPIO-NPs at 10 K and 300 K. The characteristic hysteresis was observed at 10 K and disappeared with the very negligible both remanence and coercivity at 300 K. The magnetization of the P80-TMZ/SPIO-NPs increased with a symmetric hysteresis loop when the temperature decreased to 10 K. The result indicated that the P80-TMZ/SPIO-NPs displayed the superparamagnetic characteristic and obeyed a single-domain theory above the blocking temperature, which was expected due to the very small and homogenous diameter of synthesized SPIO.

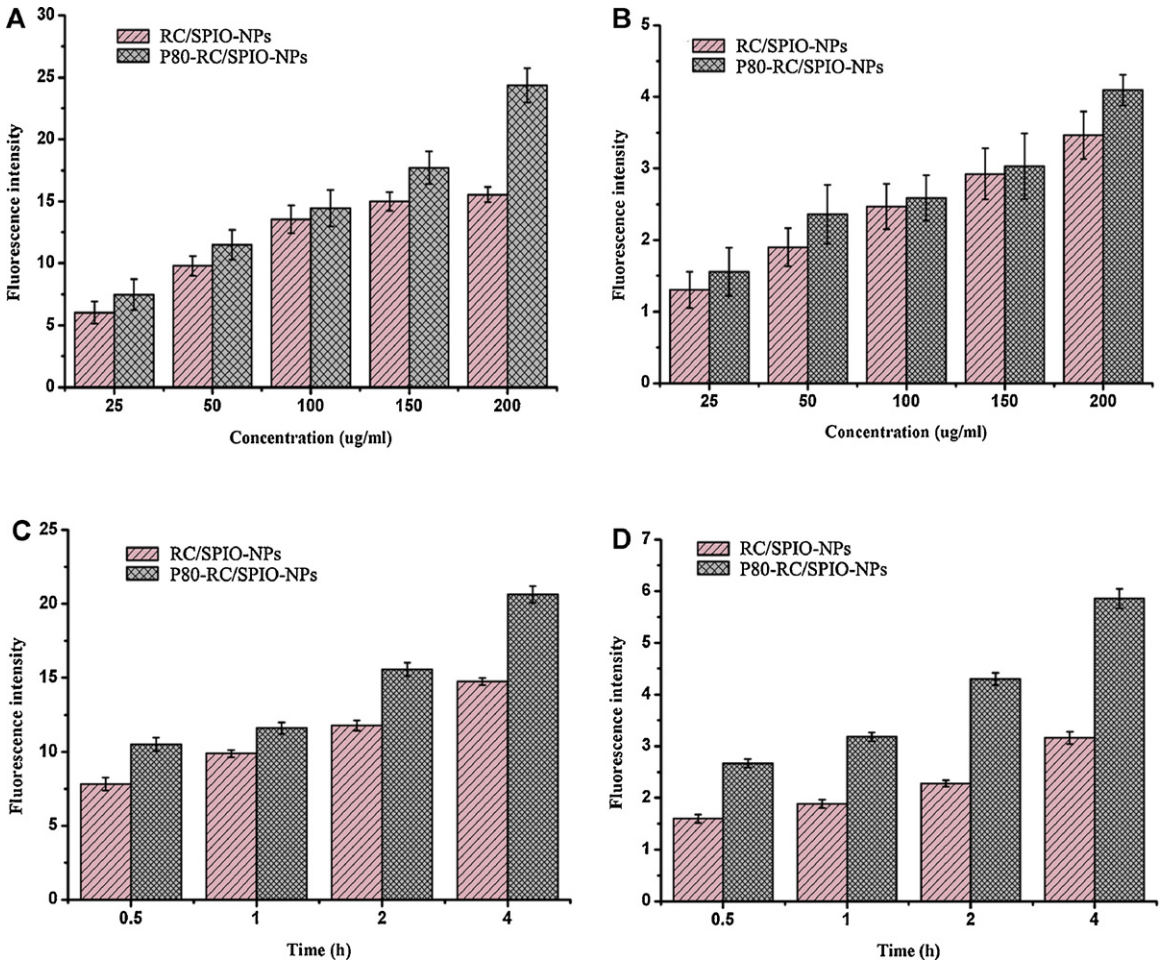

Fig. 7. The green (A) and red (B) fluorescence intensity analysis of C6 cells after 2 h incubation with previous coumarin-6 and rhodamine labeled NPs at the concentration from 25 to 200 μg/ml, respectively. The green (C) and red (D) fluorescence intensity analysis of C6 cells after incubation with previous coumarin-6 and rhodamine labeled NPs at the concentration 100 μg/ml for 0.5, 1, 2, 4 h, respectively.

3.3. *In vitro release study*

Drug-loaded carrier plays a very important role in sustained drug release in cancer therapy for enhancing the anticancer efficacy. The drug sustained release can prevent the cancer from developing drug resistance. The in vitro release profiles of TMZ were obtained by representing the percentage of TMZ release with respect to the amount of TMZ loaded in NPs. As shown in Fig. 4, the release rate of TMZ from PLGA-based NPs increased with the increase of TMZ DL amount and the period of 90% TMZ release was almost 21 days with no remarkable initial burst in the first day. Generally, the drug-loaded carriers exhibited a biphasic release pattern containing an initial burst release and a slowly sustained drug release (Kikkinides et al., 1998). The initial burst release could mostly be caused by diffusion release of drug particles surface of carriers. In our preparation of P80-TMZ/SPIO-NPs, TMZ loaded PLGA-based NPs were prepared by using emulsifying-solvent evaporation method firstly. Then the polysorbate 80 was coated on the surface of the SPIO/TMZ-NPs. This two-step progress of NPs preparation may decrease greatly the TMZ adsorption on the surface of P80-TMZ/SPIO-NPs. Thus, the drug release profiles could not appear obviously initial release in the first day. The release rate and pattern of drug from PLGA matrix is mainly dependent not only on diffusion of drug through the matrix but also on the degradation of PLGA (Fonseca et al., 2002). Therefore, drug loading amount, molecular weight, and monomer ratio of copolymer are the major factors affecting the drug release rate and pattern. A period of 90% TMZ sustained release estimated from approximately 21 days. This release pattern was mainly dependent on the diffusion of the TMZ through the polymer matrix. During the period of release, PLGA degraded progressively and formed many channels after the water uptake.

3.4. *In vitro cell investigation*

3.4.1. *Cytotoxicity assay*

The cytotoxicity of TMZ, P80-TMZ-NPs and P80-TMZ/SPIO-NPs were evaluated by the MTT assay. There was no significant difference in the toxicity of different formulations at the same drug concentrations. Therefore, our study selected 20% initial amount of TMZ loading NPs to estimate the cytotoxicity to glioma C6 cells. As shown in Fig. 4, the cytotoxicity of NPs exhibited a dose-dependent effect at TMZ concentrations from 12.5 to 400 μg/μl. On comparing the results of free TMZ after 24, 48 and 72 h incubation, the P80-TMZ/SPIO-NPs showed significant advantages in inhibiting cancer cell proliferation, good biocompatibility and no cytotoxicity against C6 cells. It has been reported that in the case of free of TM powder, all samples of different TMZ concentrations did not reveal cytotoxicity to the C6 cells after 12 h (Liu et al., 2010). The antiproliferative effect of free TMZ presented in Fig. 5 was resulted from the cell apoptosis before the 12 h and the cell proliferation of residue tolerate C6 cells after 12 h treatment. However, the TMZ loaded NPs

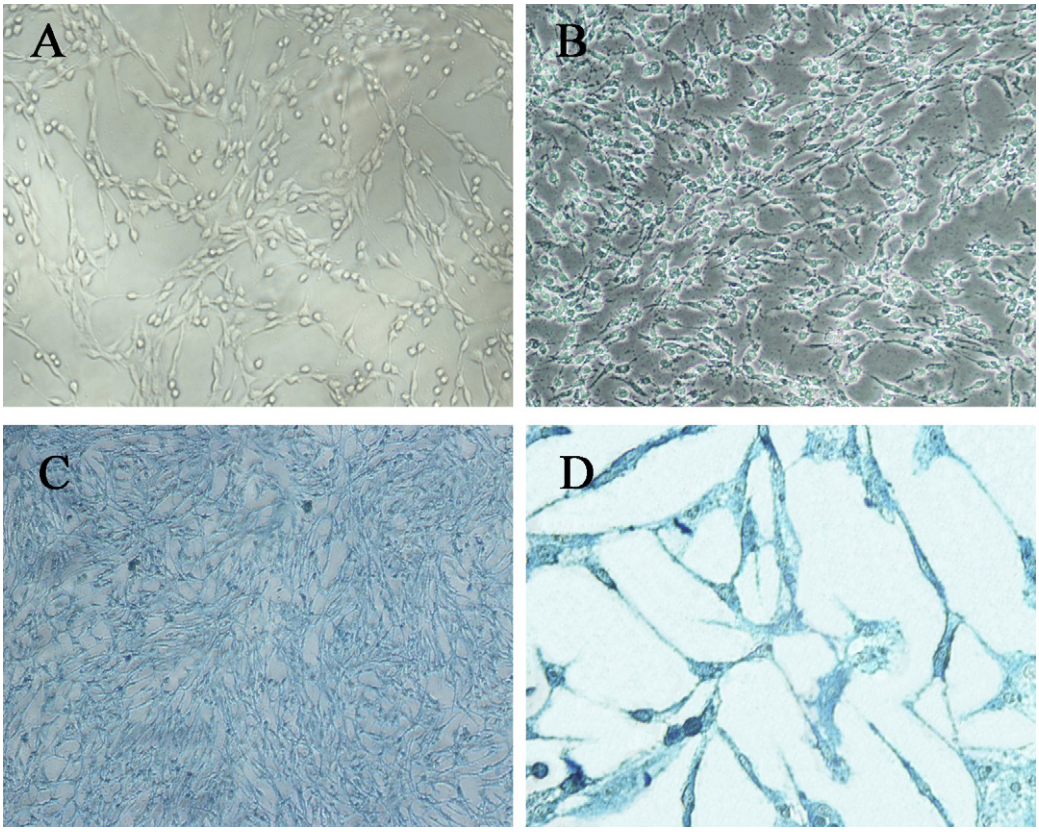

Fig. 8. Prussian blue staining images (200×) of C6 cells (2.0×10^5) after 2 h incubation with (A) P80-TMZ-NPs, (B) SPIO/TMZ-NPs and (C) P80-TMZ/SPIO-NPs at Fe concentration of 80 μg/ml; then incubated with Prussian blue liquid for 30 min. (D) The detail with enlarged scale of Prussian blue staining images (400×) incubation with P80-TMZ/SPIO-NPs at Fe concentration of 80 μg/ml for 2 h. (For interpretation of the references to color in the text, the reader is referred to the web version of the article.)

revealed higher cytotoxicity than free TMZ because of the sustained release properties.

3.4.2. Cellular uptake of NPs

Coumarin-6 and rhodamine have been widely used as probes for marking NPs in cellular uptake experiment as green and red fluorescent dye, respectively (Uddin et al., 2011; Yin et al., 2010). Fluorescence inverted microscope was used to investigate the intracellular distribution of the NPs in C6 glioma cells after 2 h incubation. P80-RC/SPIO-NPs were labeled by rhodamine and coumarin-6, and the C6 nucleus stained by blue fluorescent dye hoechst. It can be seen from Fig. 6 that the green fluorescence representing coumarin-6 labeled NPs was around the nucleus to take on a broad distribution in the cytosol while the red fluorescence representing rhodamine labeled NPs kept the same correspondence with the green fluorescence. It was demonstrated that the NPs had been internalized by the C6 cells rather than the free fluorescent dyes uptaking. Therefore, it provided feasibility for quantitative calculation cellular uptake of NPs.

For quantitative study, the NPs concentration dependence and time dependence of C6 cellular uptake effect were investigated. Firstly, P80-RC/SPIO-NPs and RC/SPIO-NPs were calculated with different NPs concentrations of 50, 100, 200, 400 μg/ml. Secondly, C6 cellular uptake efficiency of NPs was analyzed with fluorescent dye labeled NPs at concentrations 100 μg/ml for 0.5, 1, 2, 4 h, respectively. The results could be calculated either by red fluorescent dye rhodamine or by green fluorescent dye coumarin-6. However, it can be found that the tendency of the two calculation methods was consistent with each other. The cellular uptake efficiency increased with the NPs concentration increase (Fig. 7A and B). P80-RC/SPIO-NPs demonstrated higher cellular uptake efficiency for C6 glioma cells than RC/SPIO-NPs (Fig. 7C and D). The intracellular NPs concentration value of P80-RC/SPIO-NPs was 1.14, 1.17, 1.32, and 1.39-fold in comparison with RC/SPIO-NPs after 0.5, 1, 2, 4 h cell culture. It was reported that polysorbate 80 coated NPs enhanced the drug delivery efficiency and exhibited a strong dose dependent pharmacological effect for malignant tumor of brain (Kreuter et al., 1995; Alyautdin et al., 1997). Recently, Sun et al. confirmed that polysorbate 80 coating had a specific role and be necessary for the delivery of NPs into the brain (Xie et al., 2004). Borchard et al. reported that polysorbate 80 was the most efficient agent and identified as a potential "lead substance" for brain targeting (Borchard et al., 1994). Further, several mechanisms have been proposed for the transport of NPs coated with polysorbate 80 for brain targeting (Gao and Jiang, 2006; Wang et al., 2009). Similarly, our study also suggested that the higher concentration of NPs was observed in the C6 cells may be due to polysorbate 80 coating. However, the higher uptake efficiency would be further investigated in the following experiment in vivo.

3.4.3. Prussian blue staining and intracellular Fe concentration

The presence of intracellular SPIO loaded in PLGA-based NPs allowed direct visualization of their uptake by Prussian blue staining C6 cells. As shown in Fig. 8A, there was no blue color appearance in the cells incubated with P80-TMZ-NPs. Fig. 8C shows C6 cells which were incubated with the P80-TMZ/SPIO-NPs were stained in intensive blue color. Blue areas or spots could be seen in almost every cell under 80 μg/ml of the Fe concentration in culture media. Fig. 8D shows the clearer photograph of C6 cells with uptake contained NPs. The result indicated the high intracellular Fe concentration. AAS measured that the intracellular Fe concentration was 57.4 ± 3.6 μg/ml. In comparison, the C6 cells incubated with

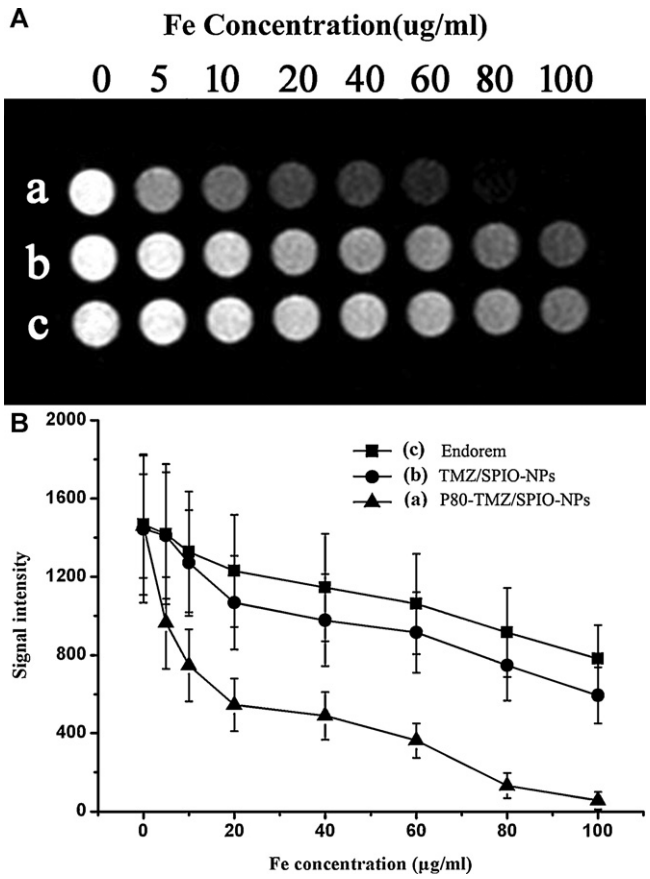

Fig. 9. T2-weighted imaging (A) and the MR signal intensity (B) of C6 cells (1×10^6) after 2 h incubation with (a) P80-TMZ/SPIO-NPs, (b) SPIO/TMZ-NPs and (c) Endorem® (a commercial contrast, Guerbet, France) at Fe concentration of 0, 5, 10, 20, 40, 60, 80, 100 μg/ml; cells were then mixed with 2% agarose solution in PBS and scanned under a 1.5 T MRI scanner (Philips Intera, Netherlands, B.V.) at room temperature.

SPIO/TMZ-NPs (Fig. 8B) showed a little weak blue color appearance. The intracellular Fe concentration was only 36.7 ± 4.8 μg/ml. Obviously, polysorbate 80 coated NPs displayed better intracellular uptake in C6 cells than non-polysorbate 80 coated NPs. The consequence was accordance with invert fluorescent microscopy.

3.5. In vitro MRI

SPIO loaded NPs with or without polysorbate 80 coated as a MRI contrast agent internalized by C6 cells in vitro were monitored by MRI. The commercial MRI contrast agent Endorem® was measured and taken for contrast experiment. As shown in Fig. 9, the MRI negatively enhanced effect of all agents in T2-weighted images and the T2 signal intensity decreased with the increasing iron concentration. Compared with T2-weighted image of the Endorem®, the T2-weighted images of cells incubated with P80-TMZ/SPIO-NPs appeared to be the darkest while that of incubated with SPIO/TMZ-NPs appeared to be darker at the same Fe concentration. The T2*w image was also scanned. However, because of too sensitive Fe particles processed by T2*w MRI sequence, T2*w images exhibited some shadow. FFE sequence scanning may be better for an investigation in vivo.

Recently, MRI has been rapidly developed particularly in accurate positioning and high resolution imaging as a non-invasive diagnostic method (Hallahan et al., 2008). However, MRI has limitation in tumor imaging for its less sensitivity. SPIO can produce predominant T2 relaxation effect and result in a signal reduction on T2-weighted images. There are two kinds of SPIO products used as MRI contrast agents in clinical diagnosis: Endorem® and Resovist® (Krestin et al., 2001). But these SPIO reagents are not applicable for tumor specific targeting because they could be quickly cleared up by phagocytic cells and accumulated in the reticuloendothelial system. A novel magnetic nanoparticle based MRI contrast agents were worth for study for researchers. Our study prepared successfully polysorbate 80 coated TMZ-loaded PLGA-based superparamagnetic NPs as a non-invasive therapeutic and diagnostic carrier. It was also demonstrated that P80-TMZ/SPIO-NPs had a good MRI negative enhance effect in C6 glioma cells MR scanning in vitro.

4. Conclusions

In this study, TMZ-loaded PLGA-based superparamagnetic NPs were successfully prepared by emulsifying-solvent evaporation method and modified by polysorbate 80 on the NPs surface. P80-TMZ/SPIO-NPs exhibited high drug loading and encapsulation efficiency as well as excellent drug sustained release performance. The glioma C6 cells experiment in vitro indicated that P80-TMZ/SPIO-NPs could be used as a novel delivery system for tumor imaging, drug delivery and real time monitoring of therapeutic effect. However, because of the cell culture limitation long-term reproductive survival of tumor clonogens could only be determined using following in vivo animal tests. It requires further studies as a multifunctional delivery system for diagnosis and treatment of brain glioma.

Acknowledgments

This work was supported by the national 973 research project of China (No. A00102110400), and the National Natural Science Foundation of China (Nos. 50732003, U0834003) and High Technology Study Plan of China (Nos. 2007AA021908, 2006AA03Z356).

References

Alyautdin, R.N., Petrov, V.E., Langer, K., Berthold, A., Kharkevich, D.A., Kreuter, J., 1997. Delivery of loperamide across the blood–brain barrier with polysorbate 80-coated polybutylcyanoacrylate nanoparticles. Pharm. Res. 14, 325–328.
Bojat, V., Baranov, D.S., Oganesyan, E.A., Hamdy, Y.M., Balaban'yan, V.Y., Alyautdin, R.N., 2011. Cytotoxic effect of paclitaxel incorporated in nanoparticles based on lactic and glycolic acid copolymer. Bull. Exp. Biol. Med. 151, 340–343.
Borchard, G., Audus, K.L., Shi, F., Kreuter, J., 1994. Uptake of surfactant-coated poly(methyl methacrylate)-nanoparticles by bovine brain microvessel endothelial cell monolayers. Int. J. Pharm. 110, 29–35.
Cheng, L., Yang, K., Li, Y.G., Zeng, X., Shao, M.W., Lee, S.T., Liu, Z., 2012. Multifunctional nanoparticles for upconversion luminescence/MR multimodal imaging and magnetically targeted photothermal therapy. Biomaterials 33, 2215–2222.
Dai, H.J., Sherlock, S.P., Tabakman, S.M., Xie, L.M., 2011. Photothermally enhanced drug delivery by ultrasmall multifunctional FeCo/graphitic shell nanocrystals. ACS Nano 5, 1505–1512.
Feng, S.S., Pan, J., 2008. Targeted delivery of paclitaxel using folate-decorated poly(lactide)—vitamin E TPGS nanoparticles. Biomaterials 29, 2663–2672.
Fessi, H., Hamoudeh, M., Al Faraj, A., Canet-Soulas, E., Bessueille, F., Leonard, D., 2007. Elaboration of PLLA-based superparamagnetic nanoparticles: characterization, magnetic behaviour study and in vitro relaxivity evaluation. Int. J. Pharm. 338, 248–257.
Fonseca, C., Simoes, S., Gaspar, R., 2002. Paclitaxel-loaded PLGA nanoparticles: preparation, physicochemical characterization and in vitro anti-tumoral activity. J. Control. Release 83, 273–286.
Gao, K., Jiang, X., 2006. Influence of particle size on transport of methotrexate across blood brain barrier by polysorbate 80-coated polybutylcyanoacrylate nanoparticles. Int. J. Pharm. 310, 213–219.
Gao, S., Zhang, H., 2007. Temozolomide/PLGA microparticles and antitumor activity against Glioma C6 cancer cells in vitro. Int. J. Pharm. 329, 122–128.
Gaya, A., Rees, J., Greenstein, A., Stebbing, J., 2002. The use of temozolomide in recurrent malignant gliomas. Cancer Treat. Rev. 28, 115–120.
Hallahan, D.E., Han, Z., Fu, A., Wang, H., Diaz, R., Geng, L., Onishko, H., 2008. Noninvasive assessment of cancer response to therapy. Nat. Med. 14, 343–349.
Huang, G., Zhang, N., Bi, X., Dou, M., 2008. Solid lipid nanoparticles of temozolomide: potential reduction of cardial and nephric toxicity. Int. J. Pharm. 355, 314–320.

Invernici, G., Cristini, S., Alessandri, G., Navone, S.E., Canzi, L., Tavian, D., Redaelli, C., Acerbi, F., Parati, E.A., 2011. Nanotechnology advances in brain tumors: the state of the art. Recent Pat. Anti-Cancer Drug Discov. 6, 58–69.

Kanwar, J.R., Mahidhara, G., Kanwar, R.K., 2009. Recent advances in nanoneurology for drug delivery to the brain. Curr. Nanosci. 5, 441–448.

Kikkinides, E.S., Charalambopoulou, G.C., Stubos, A.K., Kanellopoulos, N.K., Varelas, C.G., Steiner, C.A., 1998. A two-phase model for controlled drug release from biphasic polymer hydrogels. J. Control. Release 51, 313–325.

Kim, S., Hwang, D.W., Ko, H.Y., Lee, J.H., Kang, H., Ryu, S.H., Song, I.C., Lee, D.S., 2010. A nucleolin-targeted multimodal nanoparticle imaging probe for tracking cancer cells using an aptamer. J. Nucl. Med. 51, 98–105.

Krestin, G.P., Wang, Y.X.J., Hussain, S.M., 2001. Superparamagnetic iron oxide contrast agents: physicochemical characteristics and applications in MR imaging. Eur. Radiol. 11, 2319–2331.

Kreuter, J., Alyautdin, R.N., Kharkevich, D.A., Ivanov, A.A., 1995. Passage of peptides through the blood–brain barrier with colloidal polymer particles (nanoparticles). Brain Res. 674, 171–174.

Labhasetwar, V., Panyam, J., 2003. Biodegradable nanoparticles for drug and gene delivery to cells and tissue. Adv. Drug Deliv. Rev. 55, 329–347.

Lee, Y.M., Park, E.K., Lee, S.B., 2005. Preparation and characterization of methoxy poly(ethylene glycol)/poly(epsilon-caprolactone) amphiphilic block copolymeric nanospheres for tumor-specific folate-mediated targeting of anticancer drugs. Biomaterials 26, 1053–1061.

Ling, Y., Wei, K., Luo, Y., Gao, X., Zhong, S., 2011. Dual docetaxel/superparamagnetic iron oxide loaded nanoparticles for both targeting magnetic resonance imaging and cancer therapy. Biomaterials 32, 7139–7150.

Liu, J.M., Zhang, Y.H., Yue, Z.J., Zhang, H., Tang, G.S., Wang, Y., 2010. Temozolomide/PLGA microparticles plus vatalanib inhibits tumor growth and angiogenesis in an orthotopic glioma model. Eur. J. Pharm. Biopharm. 76, 371–375.

Neoh, K.G., Hu, F.X., Kang, E.T., 2006. Synthesis and in vitro anti-cancer evaluation of tamoxifen-loaded magnetite/PLLA composite nanoparticles. Biomaterials 27, 5725–5733.

Reni, M., Mason, W., Zaja, F., Perry, J., Franceschi, E., Bernardi, D., Dell'Oro, S., Stelitano, C., Candela, M., Abbadessa, A., Pace, A., Bordonaro, R., Latte, G., Villa, E., Ferreri, A.J.M., 2004. Salvage chemotherapy with temozolomide in primary CNS lymphomas: preliminary results of a phase II trial. Eur. J. Cancer 40, 1682–1688.

Rozhkova, E.A., 2011. Nanoscale materials for tackling brain cancer: recent progress and outlook. Adv. Mater. 23, H136–H150.

Ruan, Y., Yao, L., Zhang, B., Zhang, S., Guo, J., 2011. Antinociceptive properties of nasal delivery of Neurotoxin-loaded nanoparticles coated with polysorbate-80. Peptides 32, 1526–1529.

Suh, J.S., Lim, E.K., Huh, Y.M., Yang, J., Lee, K., Haam, S., 2011. pH-triggered drug-releasing magnetic nanoparticles for cancer therapy guided by molecular imaging by MRI. Adv. Mater. 23, 2436–2442.

Szoka, F.C., Huynh, G.H., Deen, D.F., 2006. Barriers to carrier mediated drug and gene delivery to brain tumors. J. Control. Release 110, 236–259.

Uddin, A., Lee, C.B., Wong, J., 2011. Emission properties of dopants rubrene and coumarin 6 in Alq(3) films. J. Lumin. 131, 1037–1041.

Wang, C.-X., Huang, L.-S., Hou, L.-B., Jiang, L., Yan, Z.-T., Wang, Y.-L., Chen, Z.-L., 2009. Antitumor effects of polysorbate-80 coated gemcitabine polybutylcyanoacrylate nanoparticles in vitro and its pharmacodynamics in vivo on C6 glioma cells of a brain tumor model. Brain Res. 1261, 91–99.

Wilson, B., Samanta, M.K., Santhi, K., Kumar, K.P.S., Paramakrishnan, N., Suresh, B., 2008. Targeted delivery of tacrine into the brain with polysorbate 80-coated poly(n-butylcyanoacrylate) nanoparticles. Eur. J. Pharm. Biopharm. 70, 75–84.

Xie, C.S., Sun, W.Q., Wang, H.F., Hu, Y., 2004. Specific role of polysorbate 80 coating on the targeting of nanoparticles to the brain. Biomaterials 25, 3065–3071.

Xu, H., Cheng, L., Wang, C., Ma, X.X., Li, Y.G., Liu, Z., 2011. Polymer encapsulated upconversion nanoparticle/iron oxide nanocomposites formultimodal imaging and magnetic targeted drug delivery. Biomaterials 32, 9364–9373.

Yin, C.X., Huo, F.J., Su, J., Sun, Y.Q., Tong, H.B., Nie, Z.X., 2010. A rhodamine-based dual chemosensor for the visual detection of copper and the ratiometric fluorescent detection of vanadium. Dyes Pigments 86, 50–55.

Zhang, M.Q., Sun, C., Lee, J.S.H., 2008. Magnetic nanoparticles in MR imaging and drug delivery. Adv. Drug Deliv. Rev. 60, 1252–1265.

Zhang, N., Liu, Y.J., Chen, Z.J., Liu, C.X., Yu, D.X., Lu, Z.J., 2011. Gadolinium-loaded polymeric nanoparticles modified with anti-VEGF as multifunctional MRI contrast agents for the diagnosis of liver cancer. Biomaterials 32, 5167–5176.